

Structure and dynamics of a salt-bridge model system in water and DMSO

S. Lotze^{a)} and H. J. BakkerFOM-Institute for Atomic and Molecular Physics AMOLF, Science Park 104,
1098XG Amsterdam, The Netherlands

(Received 16 February 2015; accepted 13 April 2015; published online XX XX XXXX)

We study the interaction between the ions methylguanidinium and trifluoroacetate dissolved in D₂O and dimethylsulfoxide with linear infrared spectroscopy and femtosecond two-dimensional infrared spectroscopy. These ions constitute model systems for the side groups of arginine, glutamic, and aspartic acid that are known to form salt bridges in proteins. We find that the salt-bridge formation of methylguanidinium and trifluoroacetate leads to a significant acceleration of the vibrational relaxation dynamics of the antisymmetric COO stretching vibration of the carboxyl moiety of trifluoroacetate. Salt-bridge formation has little effect on the rate of the spectral fluctuations of the CN stretching vibrations of methylguanidinium. The anisotropy of the cross peaks between the antisymmetric COO stretching vibration of trifluoroacetate and the CN stretching vibrations of methylguanidinium reveals that the salt-bridge is preferentially formed in a bidentate end-on configuration in which the two C=O groups of the carboxylate moiety form strong hydrogen bonds with the two -NH₂ groups of methylguanidinium. © 2015 AIP Publishing LLC. [<http://dx.doi.org/10.1063/1.4918904>]

I. INTRODUCTION

Salt bridges are an ubiquitous structural motive in proteins formed between amino acids with a basic side chain (histidine, lysine, or arginine), which are protonated at physiological pH conditions and hence bear a positive charge, and amino acids with an acidic side chain (aspartic/glutamic acid), which are deprotonated and hence bear a negative charge under all but the most acidic conditions. It has long been believed that the favorable coulombic interaction between the charged side chains would generally contribute to energetically stabilize the folded state of a protein over an unfolded state. However, this assumption has been challenged by the discovery of an energetically *unfavorable* salt bridge network in the arc repressor protein.¹ Since then, other possible roles for salt bridges have been discussed. A recent study showed for example that the presence for geometrically optimized salt bridges can speed up the folding of α -helical peptides,² which has led the authors to speculate if salt bridges might be involved in stabilizing intermediate or transition states during the folding process, rather than the fully folded state of a peptide.

Salt bridge interactions are often studied using model systems. Acetate is often used to mimic the natural amino acids glutamic acid (Glu) and aspartic acid (Asp), which both bear a carboxylate group in their side chain. The guanidinium cation forms a good model system for the naturally occurring amino acid arginine (Arg), which bears a guanidinium moiety in its side chain. Guanidinium and guanidinium-like moieties are strong infrared absorbers in the region of 1600 cm⁻¹ due to a mode that has mainly asymmetric CN stretching character with weak admixture of an ND₂-bending vibration.³ The asymmetric CN stretch vibration is a two-fold degenerate

mode in guanidinium, whereas in methyl-guanidinium ion (MeGd⁺), the degeneracy of this mode is broken by the methyl substitution, causing a splitting of the bands into a low-frequency band at 1585 cm⁻¹ and a high-frequency band at 1615 cm⁻¹.^{4,5} A similar splitting of the modes is also present in the side chain of the amino acid arginine. It was shown with two-dimensional infrared (2D-IR) spectroscopy that the CN stretching modes of arginine side-chains and of isolated guanidinium ions are strongly coupled and exhibit ultrafast energy transfer on a time scale of 2 ps.^{5,6}

Recently, 2DIR-spectroscopy was used for the first time to determine the structure of a salt bridge model system in dimethylsulfoxide (DMSO).⁷ From the cross-peaks resulting from mixing of the vibrational modes of guanidinium and acetate, the geometry of the complex could be inferred. Here, we use 2D-IR spectroscopy to study the salt-bridge interaction between methylguanidinium (MeGd⁺) and trifluoroacetate (TFA⁻) in D₂O and DMSO. The TFA⁻ anion exhibits sharp and intense infrared absorptions in the spectral region of 1670 to 1690 cm⁻¹ due to the asymmetric COO-stretch vibrations.⁸ TFA⁻ is a strong organic acid (pKa in water 0.23)⁹ and has found widespread use in many areas of preparative and analytical chemistry such as reversed-phase chromatography,¹⁰ mass-spectrometry,¹¹ and solid-phase synthesis of peptides.¹² Furthermore, a stabilizing effect of TFA⁻ on urea-unfolded proteins has been reported.¹³ The role of TFA⁻ in inducing conformational transitions of proteins towards a molten globule state by binding to positively charged sites and thereby minimizing intraprotein charge repulsion has been discussed.¹⁴ An effect of the presence of small amounts of TFA⁻ anions on the size and morphology of fibrils formed by β -amyloid peptides has been reported.¹⁵ By using MeGd⁺ as a model for the side chain of the amino acid arginine in combination with TFA⁻, we are able to identify the preferred binding geometry between the two ions.

^{a)}Electronic address: lotze@amolf.nl

II. EXPERIMENTAL METHODS

We study the salt-bridge interaction with the spectral hole-burning implementation of 2D-IR spectroscopy. The experimental approach has been outlined in detail elsewhere.¹⁶ In brief, we use 4.5 W of the output of a pulsed Ti:sapphire regenerative amplifier (Coherent Legend Elite Duo) to pump an optical parametric amplifier based on β -barium borate (HE-Topas, Light conversion), generating signal and idler pulses with a center wavelength around 1480 nm and 1852 nm, respectively. The signal and idler pulses are used in a subsequent difference frequency generation process in a silver thiogallate crystal (AgGaS_2 , cut-angle $\Theta = 39^\circ$) to generate mid-IR-pulses with a center wavelength of $\sim 5.9 \mu\text{m}$. The resulting mid-IR pulses have an energy of 25 μJ and a spectral width of approximately 350 cm^{-1} . Small portions ($\sim 0.3\%$) of the mid-IR pulses are split-off by means of two wedged CaF_2 -windows and used as probe and reference beams. The probe beam is sent over a motorized delay stage to vary the time delay between the pump and probe pulses. The transmitted light is used as the pump beam. The narrow-band excitation pulses ($\Delta\nu \approx 10 \text{ cm}^{-1}$) are generated from a tunable Fabry-Perot etalon in the path of the pump beam, consisting of two partially transparent mirrors ($R = 90\%$), one of which is mounted on a piezo-driven mirror mount. The ω_{pump} -axis of the 2D-IR spectra is obtained by scanning the excitation pulse over the desired spectral range, which is achieved by varying the spacing of the etalon mirrors and the spectral shape of which is controlled by closed-loop feedback.

The pump, probe, and reference beams are focused into the sample by a gold-coated off-axis parabolic mirror ($f = 75 \text{ mm}$) and recollimated by an identical mirror. The pump and probe foci are spatially overlapped in the sample. The transmitted probe and reference beams are focused onto the entrance slit of an imaging monochromator (Lot-Oriel MSH 302) with an off-axis parabolic mirror ($f = 100 \text{ mm}$) and frequency-dispersed on the two lines of a 2×32 mercury-cadmium-telluride (MCT, Infrared Associates) array. The reference beam is used for a pulse-to-pulse correction of the intensity fluctuations. The pump beam is chopped at a frequency of 500 Hz to detect the pump-induced absorption

changes in the probe light as a function of pump-probe delay. A zero-order $\lambda/2$ -plate is used to set the polarization of the pump beam at 45° relative to that of the probe light. Behind the sample cell, a rotatable wire-grid polarizer is placed to select the polarization component of the probe beam parallel or perpendicular to the pump beam. With these signals, the isotropic (rotation-free) absorption can be constructed,

$$\Delta\alpha_{\text{iso}}(\omega, t) = \frac{1}{3}(\Delta\alpha_{\parallel}(\omega, t) + 2\Delta\alpha_{\perp}(\omega, t)). \quad (1)$$

The isotropic signal is unaffected by orientational effects and reflects vibrational relaxation and spectral diffusion. In addition, we also construct the anisotropy parameter $R(\omega, t)$ that represents the orientation of the transition dipole moment of the probed vibration,

$$R(\omega, t) = \frac{\Delta\alpha_{\parallel}(\omega, t) - \Delta\alpha_{\perp}(\omega, t)}{3\Delta\alpha_{\text{iso}}(\omega, t)}. \quad (2)$$

Methylguanidinium chloride, NaTFA^- , and deuterated DMSO were obtained from Sigma-Aldrich and used without further purification. The samples were prepared by dissolving the salts in D_2O (Cambridge Isotope Laboratories, isotopic purity 99.96%). D_2O is used instead of H_2O to avoid absorption of the infrared pulses by the bending mode of H_2O around 1660 cm^{-1} .

III. RESULTS AND DISCUSSION

A. Linear absorption spectra

Figure 1 shows linear absorption spectra of solutions of MeGd^+ and TFA^- in D_2O and DMSO. The spectra show a double peak structure around 1600 cm^{-1} that can be assigned to the CN-stretching vibrations of MeGd^+ .⁶ The lower-frequency mode at 1590 cm^{-1} is associated with an antisymmetric vibration of CN bonds to the two NH_2 groups of MeGd^+ , while the higher-frequency mode at 1620 cm^{-1} is dominated by a CN stretching vibration in which the stretching of the CN bond to the NHCH_3 group is in opposite phase to the symmetric stretching of the two CN bonds to the NH_2 groups.⁶ The mode at 1620 cm^{-1} has a transition dipole moment that is oriented

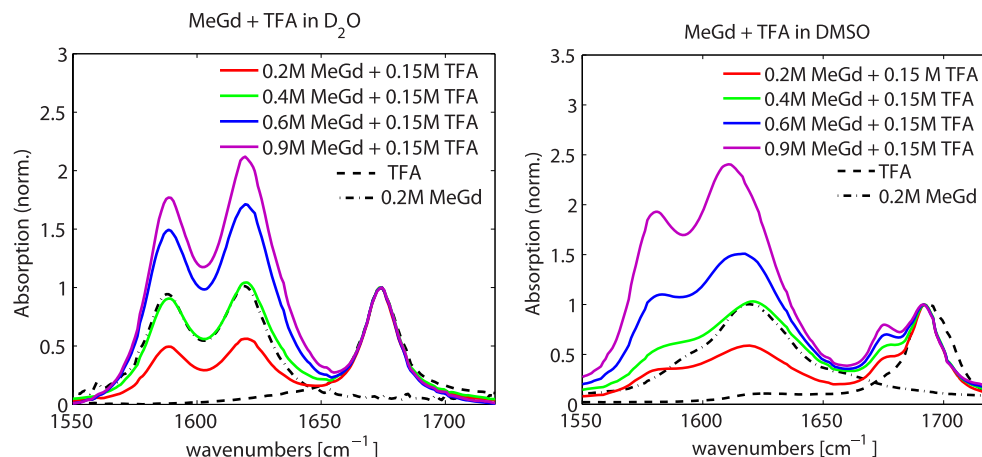


FIG. 1. FTIR-absorption spectra of MeGd dissolved in (a) D_2O and (b) DMSO. The spectra have been normalized to the COO-stretch absorption line in the $1670\text{--}1690 \text{ cm}^{-1}$ region. Absorption spectra without TFA^- have been normalized to the maximum of the CN stretching band. The spectra in panel (a) have been corrected for the broad D_2O background absorption.

close to the bisectrix of the two NH_2 groups, and the transition dipole of the mode at 1590 cm^{-1} is oriented at an angle of $\sim 100^\circ$ with respect to this bisectrix. The spectra also show a Lorentzian-shaped peak at 1690 cm^{-1} for solutions in DMSO and at 1670 cm^{-1} for solutions in D_2O . This band is assigned to the asymmetric COO-stretch vibration of the carboxylate group of TFA^- . The resonance position and the full width at half maximum (fwhm) of $\sim 16 \text{ cm}^{-1}$ are in good agreement with results from the previous studies.⁸ The addition of TFA^- to a solution of MeGd in D_2O leads to minor variation in the absorption lines, leaving the center frequencies and the linewidth of both the CN-bands and the COO-band largely unaffected. For solutions in DMSO, a strongly different behavior is observed. Most notably, in a solution containing both MeGd and TFA^- , the absorption line associated with the COO-stretch vibration acquires a double-peaked line shape. The amplitude of the lower frequency peak at 1670 cm^{-1} increases with concentration of MeGd, suggesting that this peak originates from TFA^- anions that form a hydrogen-bonded complex with MeGd⁺ cations. The high-frequency peak at 1690 cm^{-1} also exhibits a small but significant red-shift of a few wavenumbers with respect to the position of this absorption line in the absence of MeGd. Additionally, the two CN stretching modes of MeGd split further apart with increasing MeGd⁺ concentration. The features observed in the linear absorption spectra of Figure 1(a) suggest that in DMSO the MeGd⁺ cation and TFA^- anion have a strong propensity to interact and to form complexes. The double-peak structure of the antisymmetric COO stretch absorption line suggests that the strength of the interaction is bimodal, with the 1670 cm^{-1} -peak representing strongly interacting MeGd⁺- TFA^- complexes and the 1690 cm^{-1} -peak originating from rather weakly bound complexes.

B. 2D-IR spectra

In Figures 2(a)-2(f), we show 2D-IR spectra measured for a solution of 0.4 M MeGd⁺ and 0.4 M TFA^- in D_2O . Three peaks on the diagonal of the spectrum can be identified, each consisting of a negative (shown in blue) change in absorption ($\Delta\alpha$) at the fundamental frequency of the vibration and a red-shifted, positive $\Delta\alpha$ (shown in red) associated with the transition between the first and second excited state of the oscillator. Analogously to the FTIR-spectra in Figure 1, the peaks at 1590 cm^{-1} and 1620 cm^{-1} are assigned to the CN stretching vibrations of the MeGd⁺-ion (referred to as ν_{CN}^{1590} and ν_{CN}^{1620} in the following), and the most intense peak at 1670 cm^{-1} is assigned to the asymmetric COO-stretching vibration of TFA^- . The latter will be referred to as ν_{COO} . Furthermore, cross-peaks between ν_{CN}^{1590} and ν_{CN}^{1620} can be observed in the off-diagonal region of the spectrum. These can be best seen in the spectra shown in Figures 2(d)-2(f), which have been obtained under perpendicular polarization of pump and probe pulses. Additionally, cross-peaks between the ν_{COO} vibration and the CN stretching modes of MeGd⁺ can be identified, which are indicative of an interaction between the two ions.

In Figure 3, we plot the dynamics of the diagonal peaks of the isotropic 2D-IR spectrum that is constructed by adding the 2D-IR spectrum measured for parallel pump-probe

polarization to 2 times the 2D-IR spectrum measured for perpendicular polarization (Eq. (1)). The decay of the diagonal peaks reflects the vibrational relaxation dynamics. With D_2O as the solvent, the vibrational relaxation of the ν_{CN}^{1590} , ν_{CN}^{1620} , and the ν_{COO} modes all exhibit very similar vibrational relaxation time scales of $1.6 \pm 0.2 \text{ ps}$. In DMSO, the ν_{CN}^{1590} and ν_{CN}^{1620} vibrations show quite similar relaxation dynamics as in D_2O , showing time constants of 1.8 ± 0.2 and $2.1 \pm 0.3 \text{ ps}$, while the ν_{COO} bands show quite different relaxation behavior. The ν_{COO} band at 1670 cm^{-1} decays significantly faster ($T_1 = 0.9 \pm 0.1 \text{ ps}$) than the ν_{COO} band at 1690 cm^{-1} ($T_1 = 3.4 \pm 0.4 \text{ ps}$). The decay of the ν_{COO} -mode at 1670 cm^{-1} is in fact biexponential and also contains a slow decay component with a time constant of $> 10 \text{ ps}$, which we attribute to a slower thermalization of the relaxed vibrational energy. The strikingly faster decay of the ν_{COO} band at 1670 cm^{-1} compared to the ν_{COO} band at 1690 cm^{-1} band is likely the result of the presence of strong hydrogen bonds between the carboxylate group of TFA^- and the NH-groups of the MeGd⁺ cation. The formation of a strong hydrogen bond increases the anharmonic coupling of the antisymmetric COO stretch vibration to lower-frequency accepting modes (including hydrogen-bond stretch vibrations), thereby speeding up the vibrational relaxation. The observation of a fast vibrational relaxation of the ν_{COO} band at 1670 cm^{-1} is thus consistent with the assignment of the 1670 cm^{-1} band to the asymmetric COO stretch vibration of TFA^- anions in strongly bound salt bridge complexes with MeGd⁺ cations.

The reorientation dynamics of the TFA^- anions can be inferred from the dynamics of the anisotropy parameter $R(t)$ associated with the diagonal peaks in the 2D-IR-spectrum. In Figure 4, we compare the anisotropy dynamics of the ν_{COO} -mode of TFA^- anions absorbing at 1670 cm^{-1} with the anisotropy dynamics of the ν_{COO} -mode of TFA^- anions absorbing at 1690 cm^{-1} . For the ν_{COO} -mode at 1670 cm^{-1} we present the anisotropy dynamics of the induced absorption ($1 \rightarrow 2$) instead of the anisotropy dynamics of the bleaching ($0 \rightarrow 1$) because the bleaching signal of this mode partially overlaps with the $1 \rightarrow 2$ -transition (induced absorption) of the ν_{COO} -mode at 1690 cm^{-1} . We observe that the ν_{COO} -mode at 1670 cm^{-1} shows a much slower anisotropy decay than the ν_{COO} -mode at 1690 cm^{-1} . This supports our assignment of the ν_{COO} -vibrations at 1670 cm^{-1} and 1690 cm^{-1} to strongly bound and weakly bound TFA^- anions, respectively.

The 2D-IR spectral line shapes give information on the homogeneous and inhomogeneous contributions to the linewidth of the absorption bands. In the case of inhomogeneous broadening, the 2D-IR line shape is elongated along the diagonal. In Figures 2(a)-2(f), it is seen that the diagonal peak of the ν_{COO} vibration shows negligible elongation along the diagonal which implies that its vibrational line shape exhibits very little inhomogeneity already at a delay time of 1 ps. This finding agrees with the very fast, sub-picosecond decay of the frequency-frequency correlation function (FFCF) of this vibration that was reported in Ref. 8. With DMSO as solvent, the diagonal peak associated with the ν_{COO} vibration of TFA^- (Figures 2(g)-2(l)) has a complex shape resulting from the interference between different transitions associated with the two partially overlapping peaks of this band. This

292

293

294

295

296

297

298

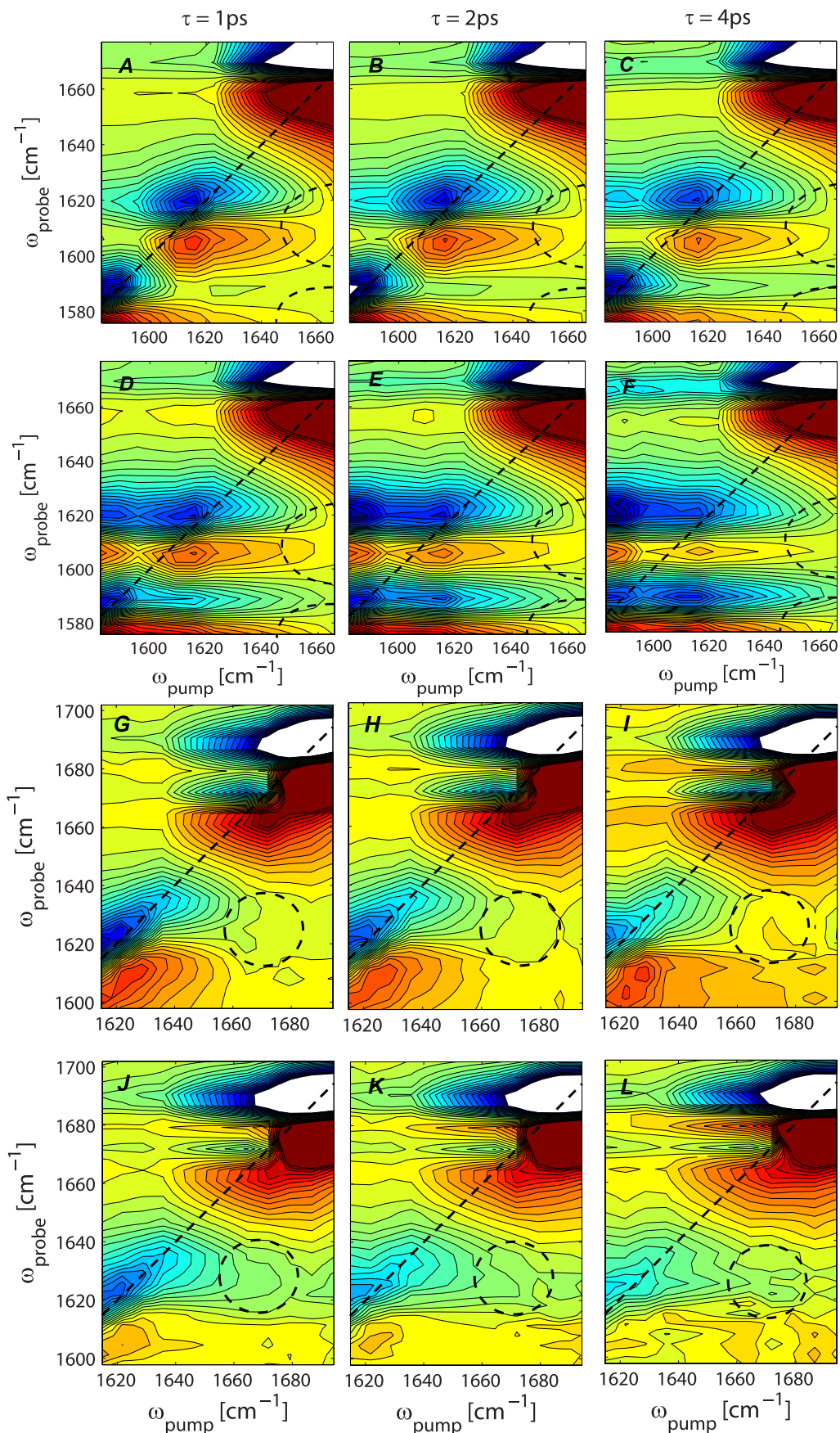
299

300

301

302

303



304 FIG. 2. 2D-IR spectra at various delay times obtained for a solution of 0.4 M MeGd^+ + 0.4 M TFA^- in D_2O ((a)-(f)) and a solution of 0.6 M MeGd^+ + 0.15 M TFA^- in DMSO ((g)-(l)). The 2D-IR spectra (a)-(c) and (g)-(i) are measured with parallel polarization of the excitation and detection pulses, and 2D-IR spectra (d)-(f) and (j)-(l) are measured with perpendicular polarization of the excitation and detection pulses. Cross-peaks between TFA^- and MeGd^+ upon excitation of the ν_{COO} -mode at 1670 cm^{-1} are indicated.

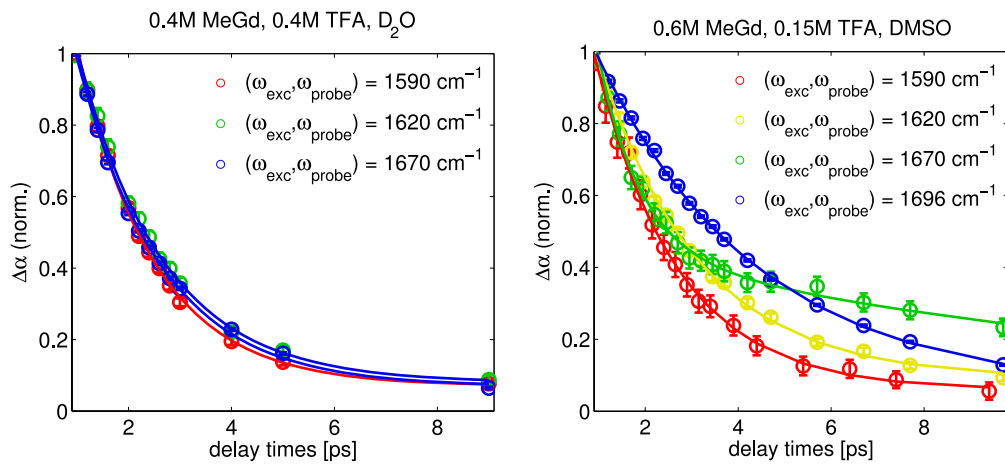
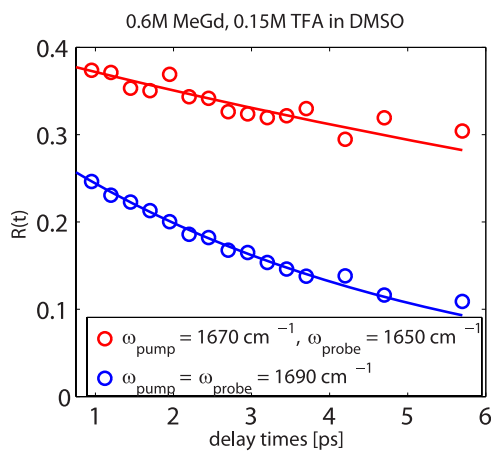
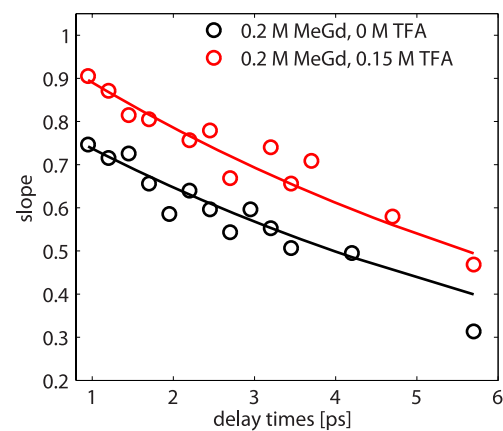


FIG. 3. Diagonal dynamics of the 2DIR-spectra in Fig. 2. The solid lines are fits of a mono-exponential decay (with a constant offset) to the data points.

complex shape also shows little elongation along the diagonal, which implies that the ν_{COO} vibration also shows little inhomogeneity when TFA^- is dissolved in DMSO.

The diagonal peaks of the ν_{CN}^{1590} and ν_{CN}^{1620} resonances of MeGd^+ also show little inhomogeneity when MeGd^+ is dissolved in D_2O (Figures 2(a)-2(f)). The observed 2D-IR line shapes are nearly parallel to the pump-axis of the spectrum. This observation is in agreement with the ~ 1 ps — decay time reported in Ref. 5 for the FFCF of Gdm^+ in D_2O . In this work, the apparent ultrafast spectral diffusion processes were attributed to the rapid reconfigurations of the solvation shell around the ion. In contrast, the spectra obtained for a solution of MeGd^+ in DMSO (Figures 2(g)-2(l)) show a strong elongation of the diagonal peak associated with the ν_{CN}^{1620} -mode along the diagonal of the spectrum that is not fully decayed at a delay time of 4 ps (Figure 2(i)). A similar diagonal elongation is also observed for the ν_{CN}^{1590} -mode in the 2D-IR-spectra shown in the supplementary material, where the ω_{pump} - and ω_{probe} -axes extend to lower frequencies.¹⁷ Hence, spectral diffusion is much slower in DMSO than in D_2O .

To quantify the spectral diffusion dynamics, we determined the delay dependence of the center line slope, i.e., the slope of the line that connects the frequency positions of the maxima of the negative absorption changes obtained at different excitation frequencies ω_{pump} . Plotting this slope as a function delay time reflects the decay of the frequency-frequency correlation function.¹⁸ In Figure 5, we present the results of this analysis for the ν_{CN}^{1620} vibration of MeGd in DMSO, both in the presence and in the absence of TFA^- . The center line slope of ν_{CN}^{1620} is found to show a decay with a time-constant of 7.5 ± 1 ps both in the presence and in the absence of TFA^- . The slightly higher starting value seen in Figure 5 in the presence of TFA^- indicates that the formation of salt bridges increases the width of the frequency distribution of the ν_{CN}^{1620} vibration. The insensitivity of the spectral diffusion dynamics with respect to the addition of TFA^- shows that the spectral fluctuations likely result from interactions with surrounding DMSO solvent molecules that show little dependence on the presence of the salt bridge. This explanation is in line with the fact that the ν_{CN}^{1620} line shape is near homogeneous in D_2O , where the interactions with the light D_2O molecules are expected to fluctuate on a much shorter time scale. It

FIG. 4. Comparison of the dynamics of the anisotropy parameter $R(t)$ of the bleaching signal of the diagonal peak associated with weakly bound TFA^- anions at $\omega_{\text{pump}} = \omega_{\text{probe}} = 1690 \text{ cm}^{-1}$ (blue circles) and the induced absorption signal of the diagonal peak of the strongly bound TFA^- anions at $\omega_{\text{pump}} = 1670 \text{ cm}^{-1}$ and $\omega_{\text{probe}} = 1650 \text{ cm}^{-1}$ (red circles). The solid lines are mono-exponential fits.FIG. 5. Central line slope as a function of delay time for the symmetric CN stretching mode of MeGd^+ at 1620 cm^{-1} . Black symbols show the data obtained for a solution of 0.2 M MeGdCl in DMSO, and red symbols represent the data obtained for a solution of 0.2 M MeGdCl and 0.15 M NaTFA^- in DMSO.

should be noted that, due to the spectrally narrow bandwidth of the excitation pulses in our experiment, we cannot resolve the dynamics occurring on time scales shorter than ~ 1 ps. Hence, the frequency-frequency correlation of the ν_{CN}^{1620} -mode of MeGd^+ -ions embedded in a salt-bridge complex may in fact contain an additional subpicosecond component.

C. Cross-peak anisotropy of the 2D-IR spectra

The anisotropy of the cross-peaks in the 2DIR-spectrum reveals the relative orientation of the transition dipole moments of the excited and probed vibrations.^{7,19-21} The dashed line in Figs. 6 and 7 is a weighted average of a subset of the anisotropy values within a given frequency range. In this weighted average, only anisotropy data points that correspond to a certain minimum isotropic signal (the value is given in the figure captions) have been included, since the anisotropy value is no longer reliable in case the isotropic signal is close to zero. In Figure 6, we show the frequency dependence of the anisotropy parameter $R(\omega)$ at 1 ps delay time upon selective excitation of the ν_{CN}^{1590} mode and the ν_{CN}^{1620} mode of MeGd^+ . The isotropic spectra (solid lines) clearly show that excitation

of either modes leads to a response of the other mode. This off-diagonal response shows that the two modes are coupled. Both the transient spectra and the frequency dependent anisotropy values are very similar for solutions in D_2O (Figures 6(a) and 6(c)) and DMSO (Figures 6(b) and 6(d)), which implies that the intramolecular coupling between the ν_{CN}^{1590} mode and the ν_{CN}^{1620} mode is largely unaffected by interactions with the solvent.

In the diagonal region (same mode excited and probed), the anisotropy ranges between 0.3 and 0.4, which shows that there is very little reorientational motion in the first picosecond after the excitation. In the off-diagonal region, the anisotropy parameter $R(\omega)$ has a negative value around -0.05 . The value of the off-diagonal anisotropy can be related to the angle θ between the transition dipoles using the relation $R = \frac{1}{3}(3\cos^2\theta - 1)$. We infer an angle of $120^\circ \pm 5^\circ$ between the transition dipole moments of the two modes, which is somewhat higher than the value of 115° that was reported in Ref. 6 for arginine. The angle of 120° agrees well with the assignment of the ν_{CN}^{1590} mode to an antisymmetric vibration of the CN bonds to the two NH_2 groups of MeGd^+ and of the ν_{CN}^{1620} mode to an antisymmetric stretching of the CN bond to

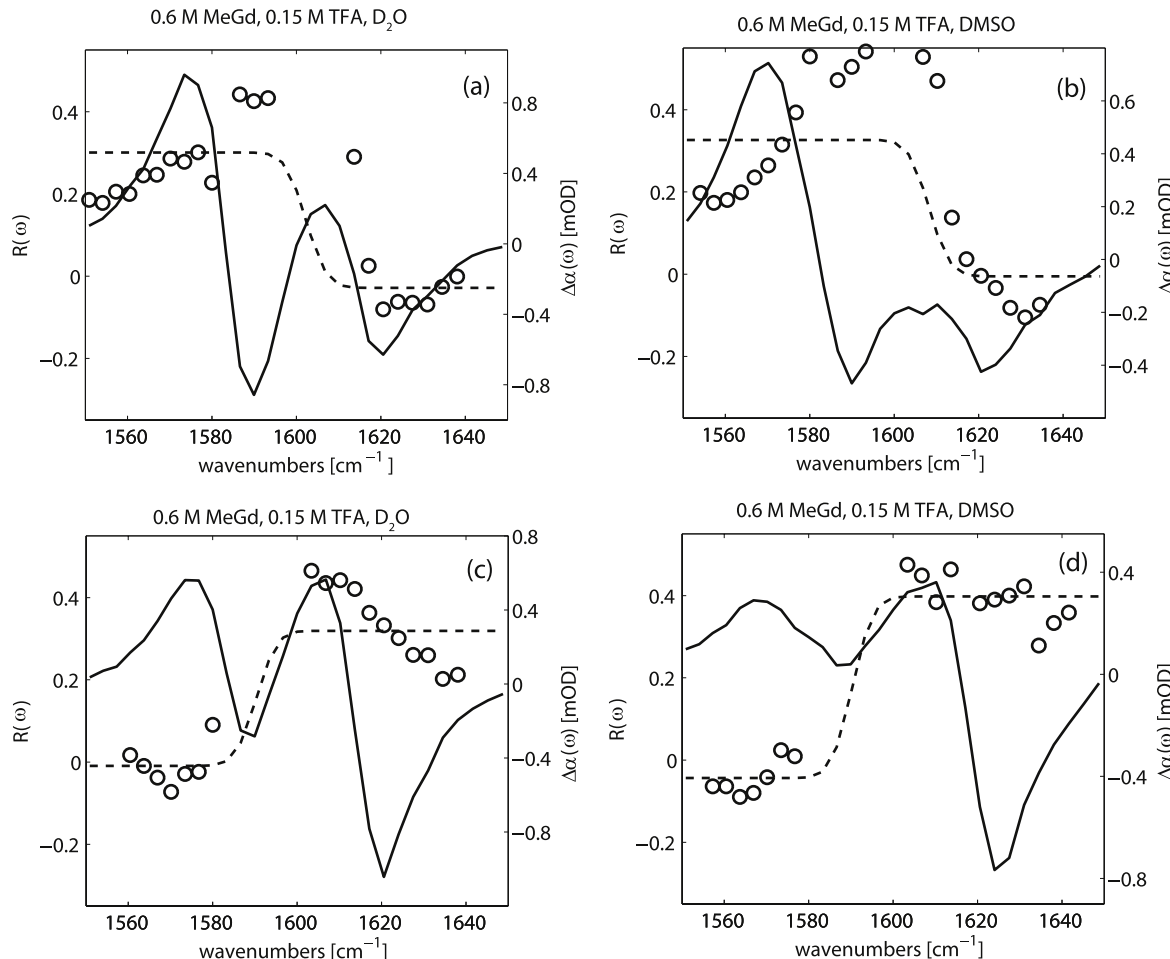


FIG. 6. Cuts through the CN stretching region of 2D-IR spectra at a delay time of 1 ps after excitation of the ν_{CN}^{1590} mode of MeGd^+ ((a) and (b)) and of the ν_{CN}^{1620} mode ((c) and (d)) of MeGd^+ , measured for a solution of 0.6 M MeGdCl and 0.15 M NaTFA^- in D_2O ((a) and (c)) and DMSO ((b) and (d)). The symbols denote the frequency dependent anisotropy $R(\omega)$ (left vertical axis), and the solid lines represent the isotropic transient spectrum (right vertical axis). The dashed line is a weighted average of the anisotropy values of the diagonal and cross-peaks. Only anisotropy data points that correspond to an isotropic signal $\Delta\alpha_{iso} > 0.15$ mOD have been included.

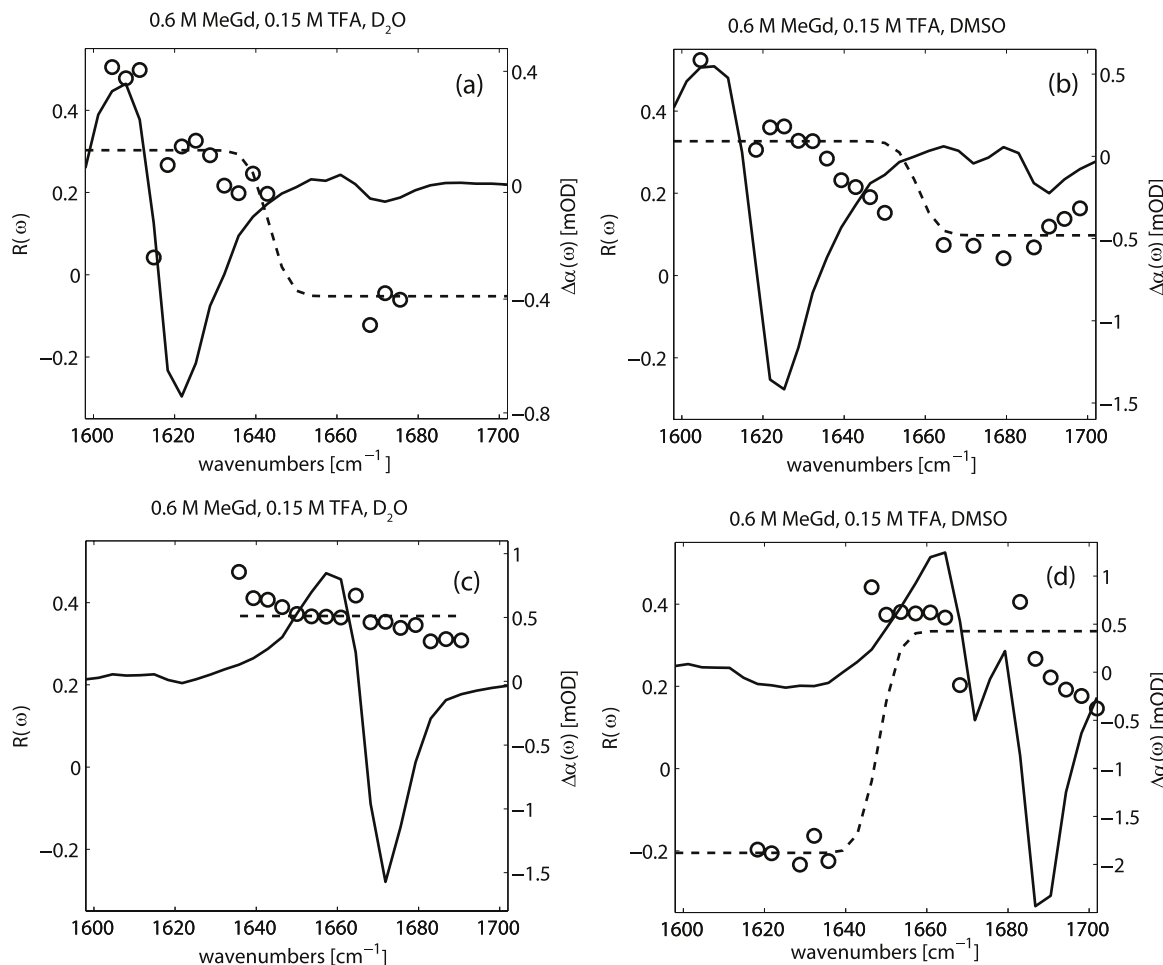


FIG. 7. Cuts through the 2D-IR spectra at 1 ps delay time after excitation of the ν_{CN}^{1620} mode of MeGd^+ ((a) and (b)) and the ν_{COO} mode at 1670 cm^{-1} of TFA^- ((c) and (d)), measured for a solution of 0.6 M MeGdCl and 0.15 M NaTFA^- in D_2O ((a) and (c)) and DMSO ((b) and (d)). The symbols denote the frequency dependent anisotropy $R(\omega)$ (left vertical axis), and the solid lines represent the isotropic transient spectrum (right vertical axis). The dashed line is a weighted average of the anisotropy values of the diagonal and cross-peaks. Only anisotropy data points that correspond to an isotropic signal $\Delta\alpha_{iso} > 0.05 \text{ mOD}$ have been included.

the NHCH_3 group with respect to the symmetric stretching of the two CN bonds to the two NH_2 groups.⁶

In Figure 7, we show the transient spectra and anisotropy values over a frequency range that encompasses both the CN stretching vibrations of MeGd^+ and the COO-stretching vibrations of TFA^- . Excitation of the ν_{CN}^{1620} or the ν_{COO} band at 1670 cm^{-1} gives a clear cross-peak response at the other type of modes due to the formation of a salt bridge between MeGd^+ and TFA^- . The cross-peaks in the $1670\text{--}1690 \text{ cm}^{-1}$ region for $\omega_{pump} = 1620 \text{ cm}^{-1}$ are more pronounced for a solution in DMSO (Figure 7(b)) than for a solution in D_2O (Figure 7(a)). This result is not unexpected as DMSO has a lower dielectric constant than water ($\epsilon_{DMSO} = 48$, $\epsilon_{water} = 80$), which leads to a stronger coulombic attraction between the two oppositely charged ions. Hence, MeGd^+ and TFA^- show a higher propensity to form salt-bridge complexes in DMSO than in D_2O . Excitation of the ν_{CN}^{1620} mode of MeGd^+ in DMSO leads to two distinct cross-peaks at $\omega_{probe} = 1670 \text{ cm}^{-1}$ and $\omega_{probe} = 1690 \text{ cm}^{-1}$ which shows that both ν_{COO} modes are coupled to the ν_{CN}^{1620} mode (Figure 7(b)). The observation of both ν_{COO} modes at 1670 cm^{-1} and 1690 cm^{-1} following excitation of ν_{CN}^{1620} shows

that both ν_{COO} bands contain contributions from hydrogen-bonded complexes of MeGd^+ and TFA^- . This points at a bimodal distribution of binding strengths.

Salt bridges exist in different binding geometries in proteins. In a bidentate binding geometry, both C=O groups of a carboxylate moiety are hydrogen bonded to two N-H groups of a guanidinium moiety, whereas in a monodentate configuration, only a single C=O group and a single N-H group form a hydrogen bond. In general, the salt-bridge interaction between arginine and aspartic or glutamic acid has a prevalence for a bidentate configuration.²² There are two possible configurations for this bidentate binding interaction. The two C=O groups can either bind to two NH_2 -groups of the guanidinium-moiety (end-on) or bind to an NH_2 group and the NHR group that includes the alkyl R substituent (side-on).²² The salt-bridge configuration in proteins will strongly depend on steric effects. For instance, it has been found with 2D-IR spectroscopy that a bidentate geometry is preferred in a model β -turn polypeptide, whereas a monodentate configuration is preferred in a model α -helical peptide.²³ The geometry of the salt bridge formed between MeGd^+ and TFA^- can be derived from the polarization-resolved 2D-IR spectra of Figure 2.

The anisotropy of the ν_{COO} mode following excitation of the ν_{CN}^{1620} mode has a value close to zero (Figures 7(a) and 7(b)). This finding shows that the response of the ν_{COO} modes is dominated by cross-anharmonic coupling between the ν_{CN}^{1620} and ν_{COO} modes and not the result of direct excitation of the very low-frequency wing of the absorption band of the ν_{COO} vibrations, as this would result in a value of $R(\omega)$ of ~ 0.4 . The small value of the anisotropy indicates that the transition dipole moments of the ν_{CN}^{1620} and ν_{COO} modes are oriented at a large relative angle. For solutions of MeGd^+ and TFA^- in D_2O , the signal of the ν_{CN}^{1620} mode following excitation of the ν_{COO} mode is very weak (Figure 7(c)), thus preventing an accurate determination of its anisotropy. The weak signal of the cross peak indicates that there exists a large fraction of free (uncomplexed) TFA^- in D_2O .

Excitation of the ν_{COO} mode at 1670 cm^{-1} for a solution of MeGd^+ and TFA^- in DMSO yields a clear cross-peak signal at the ν_{CN}^{1620} mode with an anisotropy value of $R(\omega) = -0.2$ (Figure 7(d)). Excitation of the ν_{COO} mode at 1670 cm^{-1} in DMSO exclusively excites TFA^- molecules forming salt-bridge complexes. Hence, the contribution of directly excited ν_{COO} modes to the signal measured in the frequency range of the ν_{CN}^{1620} mode will be smaller than in the case of Figure 7(b), where the signal measured in the frequency region of the ν_{COO} modes also has a significant contribution of uncomplexed TFA^- anions at the given stoichiometry of $\text{MeGd}^+:\text{TFA}^- = 4:1$. The excitation of the CN-mode at 1620 cm^{-1} is therefore *not* only selective for MeGd^+ ions in salt-bridge complexes but also involves the excitation of unbound MeGd^+ ions. This latter species does not give rise to a cross-peak signal at 1670 cm^{-1} , but its high-frequency wing gives rise to a transient absorption change in the 1670 cm^{-1} -region. This signal will have a high ($R = 0.4$) anisotropy value and adds to the low anisotropy ($R = -0.2$) expected for the ($\omega_{pump} = 1620 \text{ cm}^{-1}$ and $\omega_{probe} = 1670 \text{ cm}^{-1}$)-cross-peak, resulting in the intermediate anisotropy value of $R = 0.1$ that is observed in Fig. 7(b). Since the 1670 cm^{-1} -peak results exclusively from TFA^- anions in salt-bridge complexes, the aforementioned effect does not affect the anisotropy of the ($\omega_{pump} = 1670 \text{ cm}^{-1}$ and $\omega_{probe} = 1620 \text{ cm}^{-1}$)-cross-peak, making the anisotropy in Fig. 7(d) a reliable measure for the angle between the transition dipoles of the COO-stretch vibration and the CN-stretch vibration in a salt-bridge complex.

For the cross-peak of the ν_{COO} -mode around 1690 cm^{-1} and the ν_{CN}^{1620} -mode, originating from weakly bound salt bridge complexes, we also observe a value of $R = -0.2$ (Fig. 8). It can be excluded that the cross-peak in the region of the ν_{CN}^{1620} -vibration originates from excitation of the high frequency wing of the ν_{COO} -vibration of strongly bound TFA^- anions based on the absence of any bleaching-like feature 1670 cm^{-1} in the isotropic transient spectrum of Fig. 8. In Fig. 9, we present the dynamics of the cross-peak around $\omega_{probe} = 1620 \text{ cm}^{-1}$ upon excitation of the ν_{COO} -mode at 1670 cm^{-1} . The anisotropy shows little time dependence (within the experimental uncertainty) up to a delay time of 5 ps, indicating that the reorientation is a quite slow process, in agreement with the observation of the slow decay of the anisotropy of the diagonal ν_{COO} -peak at 1670 cm^{-1} in Fig. 4.

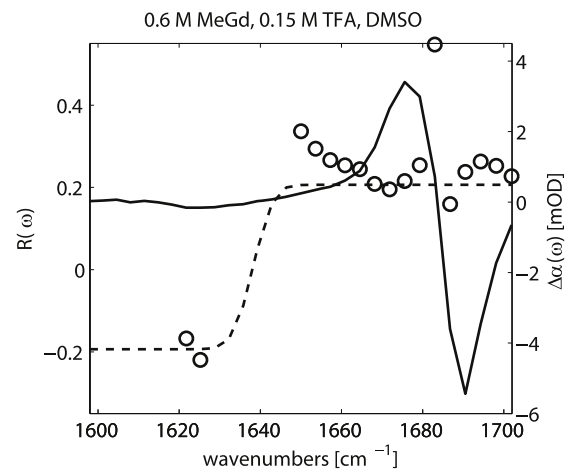


FIG. 8. Cuts through the 2D-IR spectra at 1 ps delay time after excitation of the ν_{COO} mode of weakly bound TFA^- anions at 1690 cm^{-1} measured for a solution of 0.6 M MeGdCl and 0.15 M NaTFA^- in DMSO. The symbols denote the frequency dependent anisotropy $R(\omega)$ (left vertical axis), and the solid lines represent the isotropic transient spectrum ($\Delta\alpha(\omega)$, right vertical axis). The cross-peak anisotropy of $R \approx -0.2$ suggests that weakly bound salt bridge complexes between MeGd^+ and TFA^- also adopt an end-on geometry, similar to the strongly bound complexes.

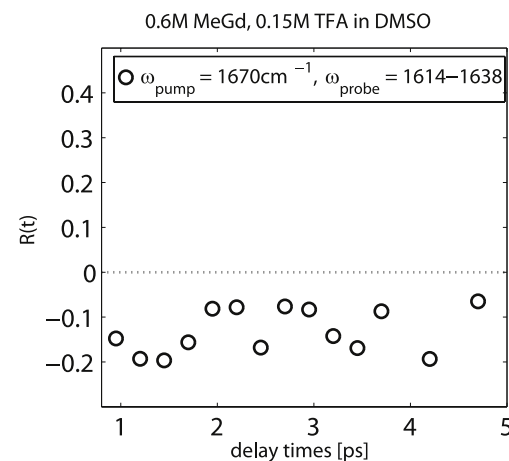


FIG. 9. Time-dependence of the cross-peak anisotropy associated with the ν_{CN}^{1620} -mode upon excitation of the ν_{COO} - 1670 cm^{-1} -mode. Each data point has been obtained by averaging along the ω_{probe} -axis from 1614 to 1638 cm^{-1} .

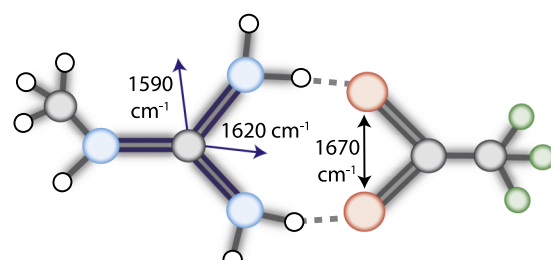


FIG. 10. Geometry of the salt bridge formed between MeGd^+ and the TFA^- -anion as inferred from the polarization-resolved 2D-IR spectrum. The cross-peak anisotropy values indicate that the complex adopts a bidentate end-on geometry, with the carboxylate-group of TFA^- binding to the two NH_2 -groups of the MeGd^+ cation. Arrows depict the transition dipoles of the CN stretching modes of MeGd^+ and the ν_{COO} mode of the TFA^- -anion.

An anisotropy value of $R(\omega) = -0.2$ corresponds to a relative angle of 90° between the transition dipole moments of the ν_{COO} and ν_{CN}^{1620} modes. The results of Figures 7(a), 7(b), 7(d), and 8 thus show that the transition dipole moments of ν_{CN}^{1620} , and the antisymmetric ν_{COO} vibrations have a nearly perpendicular orientation in the salt-bridged complexes of MeGd^+ and TFA^- . This finding indicates a geometric arrangement as outlined in Figure 10. The carboxylate group of the TFA^- -anion binds in a bidentate end-on configuration to the two NH_2 -groups of the MeGd^+ cation.

IV. CONCLUSIONS

We study the interaction between MeGd^+ and TFA^- in D_2O and DMSO using linear infrared spectroscopy and femtosecond 2D-IR spectroscopy. For methylguanidinium, we probe the CN stretching vibrations at 1590 and 1620 cm^{-1} ; for TFA^- , we probe the antisymmetric COO stretching vibration with a frequency of 1670 cm^{-1} in D_2O and frequencies of 1670 cm^{-1} and 1690 cm^{-1} in DMSO. We find that in both solvents MeGd^+ and TFA^- have a strong tendency to form salt-bridge complexes in which the $\text{C}=\text{O}$ groups of TFA^- from strong hydrogen bonds to two N-H groups of MeGd^+ .

In DMSO, the formation of the salt bridge leads to a strong acceleration of the vibrational relaxation of the antisymmetric COO vibration of TFA^- , from $3.4 \pm 0.4\text{ ps}$ to $0.9 \pm 0.1\text{ ps}$. Salt bridge formation has little effect on the time constant of vibrational relaxation of the CN stretching vibrations. Both CN stretching vibrations at 1590 and 1620 cm^{-1} have a vibrational relaxation time of $\sim 2\text{ ps}$, irrespective of the solvent or salt-bridge formation. In DMSO, the CN stretching vibrations show quite slow spectral diffusion with a time constant of $7.5 \pm 1\text{ ps}$. This time constant is the same for isolated MeGd^+ and for MeGd^+ contained in a salt-bridge complex, showing that the spectral fluctuations are governed by intermolecular interactions with the DMSO solvent molecules. This result is consistent with the observation that the spectral diffusion is much faster in D_2O where the interactions with the light D_2O molecules fluctuate on a much shorter time scale.

The anisotropy of the cross peaks of the 2D-IR spectrum show that the transition dipole moments of the two CN stretching vibrations at 1590 and 1620 cm^{-1} have a relative angle of 120° , which agrees with an assignment of the 1590 cm^{-1} mode to an antisymmetric vibration of the CN bonds to the two NH_2 groups of MeGd^+ and of the 1620 cm^{-1} mode to a stretching

of the CN bond to the NHCH_3 group that is in opposite phase to the symmetric stretching of the two CN bonds to the NH_2 groups.⁶ From the anisotropy values of the cross peaks of the CN stretching vibration at 1620 cm^{-1} and the antisymmetric ν_{COO} mode of TFA^- , it follows that the transition dipole moments of these vibrations have a relative orientation that is close to perpendicular. This result shows that the salt-bridge complex of MeGd^+ and TFA^- has a preferred bidentate end-on configuration in which the two $\text{C}=\text{O}$ groups of TFA^- form strong hydrogen bonds to the two NH_2 groups of MeGd^+ (Figure 10).

¹C. D. Waldburger, J. F. Schildbach, and R. T. Sauer, *Nat. Struct. Biol.* **2**, 122 (1995).

²H. Meuzelaar, M. Tros, A. Huerta-Viga, C. N. van Dijk, J. Vreede, and S. Woutersen, *J. Phys. Chem. Lett.* **5**, 900 (2014).

³R. J. Sension, B. Hudson, and P. R. Callis, *J. Phys. Chem.* **94**, 4015 (1990).

⁴D. Y. Vorobyev, C.-H. Kuo, J.-X. Chen, D. G. Kuroda, J. N. Scott, J. M. Vanderkooi, and R. M. Hochstrasser, *J. Phys. Chem. B* **113**, 15382 (2009).

⁵D. Y. Vorobyev, C.-H. Kuo, D. G. Kuroda, J. N. Scott, J. M. Vanderkooi, and R. M. Hochstrasser, *J. Phys. Chem. B* **114**, 2944 (2010).

⁶A. Ghosh, M. J. Tucker, and R. M. Hochstrasser, *J. Phys. Chem. A* **115**, 9731 (2011).

⁷A. Huerta-Viga, S. R. Domingos, S. Amirjalayer, and S. Woutersen, *Phys. Chem. Chem. Phys.* **16**, 15784 (2014).

⁸D. G. Kuroda, D. Y. Vorobyev, and R. M. Hochstrasser, *J. Chem. Phys.* **132**, 044501 (2010).

⁹J. B. Milne and T. J. Parker, *J. Solution Chem.* **10**, 479 (1981).

¹⁰G. Winkler, P. Wolschann, P. Briza, F. X. Heinz, and C. Kunz, *J. Chromatogr. A* **347**, 83 (1985).

¹¹A. Appfel, S. Fischer, G. Goldberg, P. C. Goodley, and F. E. Kuhlmann, *J. Chromatogr. A* **712**, 177 (1995), montreux symposium on liquid chromatography-mass spectrometry, supercritical fluid chromatography mass spectrometry, capillary electrophoresis-mass spectrometry and tandem mass spectrometry.

¹²D. S. King, C. G. Fields, and G. B. Fields, *Int. J. Pept. Protein Res.* **36**, 255 (1990).

¹³V. Dötsch, G. Wider, G. Siegal, and K. Wüthrich, *FEBS Lett.* **366**, 6 (1995).

¹⁴Y. Goto, N. Takahashi, and A. L. Fink, *Biochemistry* **29**, 3480 (1990).

¹⁵C. Shen, M. Fitzgerald, and R. Murphy, *Biophys. J.* **67**, 1238 (1994).

¹⁶S. Lotze, L. L. C. Olijve, I. K. Voets, and H. J. Bakker, *J. Phys. Chem. B* **118**, 8962 (2014).

¹⁷See supplementary material at <http://dx.doi.org/10.1063/1.4918904> for 2d-IR-spectra, where the ω_{pump} - and ω_{probe} -axes extend to lower frequencies.

¹⁸K. Kwak, S. Park, I. J. Finkelstein, and M. D. Fayer, *J. Chem. Phys.* **127**, 124503 (2007).

¹⁹P. Hamm, M. Lim, W. F. DeGrado, and R. M. Hochstrasser, *Proc. Natl. Acad. Sci. U. S. A.* **96**, 2036 (1999).

²⁰S. Woutersen and P. Hamm, *J. Phys. Chem. B* **104**, 11316 (2000).

²¹M. T. Zanni, N.-H. Ge, Y. S. Kim, and R. M. Hochstrasser, *Proc. Natl. Acad. Sci. U. S. A.* **98**, 11265 (2001).

²²J. E. Donald, D. W. Kulp, and W. F. DeGrado, *Proteins: Struct., Funct., Bioinf.* **79**, 898 (2011).

²³A. Huerta-Viga, S. R. Domingos, H. Meuzelaar, A. Rupenyan, and S. Woutersen, *J. Chem. Phys.* **142**, 000000 (2015).

624
625
626
627
628
629
630
631
632
633
634
635
636
637
638
639
640
641
642
643
644
645
646
647
648
649
650
651
652
653
654
655
656
657
658
659
660
661
662
663
664
665
666

667
668
669
670
671
672
673
674
675
676
677
678
679
680
681
682
683
684
685
686
687
688
689
690
691
692
693
694
695
696
697
698
699
700
701
702
703
704
705
706
707
708
709
710
711
712
713
714
715
716
717
718
Q3
Q4